1

Supramolecular Construction of Bidentate Ligands Through Self-assembly by Hydrogen Bonding

Felix Bauer and Bernhard Breit

University of Freiburg, Insitute for Organic Chemistry, Fakultät für Chemie und Pharmazie, Albertstraße 21, 79104 Freiburg, Germany

1.1 Introduction

In classical transition metal catalysis, phosphine ligands have a dominant position in controlling catalysts activity and selectivity [1, 2]. Monodentate phosphine ligands show in many catalytic transformations higher catalytic activity but lower selectivity. In contrast, bidentate ligands in which two phosphorus donors are combined by a covalent backbone often show superior selectivity in many transformations. Some of these bidentate ligands were designed to achieve high selectivity in a specific reaction. However, a disadvantage is their often lower activity compared with monodentate ligands. Moreover, the synthesis of these ligands is in most cases complicated involving a multistep route to the target ligand. This is especially a drawback in the synthesis of nonsymmetrical bidentate ligands equipped with two different donor sites.

In order to overcome these limitations, supramolecular chemistry offers a powerful tool [3–5]. In this conceptually new approach, structurally less complicated monodentate ligands might self-assemble into a bidentate coordination mode in a transition metal complex by noncovalent interactions. Nature provides many noncovalent interactions such as van der Waals interactions, π-stacking, electrostatic interactions, coordinative interactions, or hydrogen bonding [3]. Among them probably the most prominent interaction is hydrogen bonding, highlighted especially in DNA where they connect the single strands of the double helix [3, 6]. This feature can be seen as an inspiration to replace covalent bonds in the backbone of a bidentate ligand (Scheme 1.1).

The high potential of this approach is beyond a simplified ligand design and lies in the inherent possibility to generate a combinatorial ligand library through simple mixing of two ligands. This means if two different ligands are coordinated to one transition metal center from n different monodentate donor ligands, a catalyst library with $(n^2 + n)/2ML^xL^y$ could be obtained (Table 1.1).

On the other hand, when the interaction between two ligands bound to one metal center is noncomplementary, a mixture of two homodimeric and one heterodimeric

Supramolecular Catalysis: New Directions and Developments, First Edition.
Edited by Piet W.N.M. van Leeuwen and Matthieu Raynal.

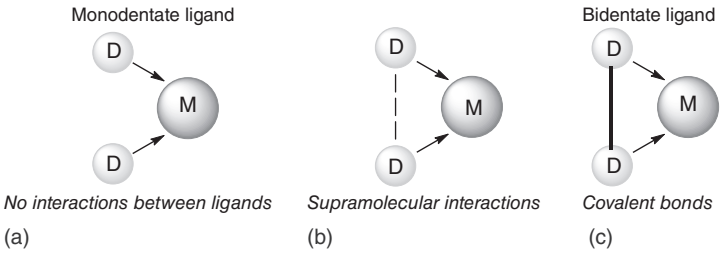

Scheme 1.1 Classical monodentate (a) and bidentate (c) ligands with a covalent-bonded backbone; self-assembled bidentate ligand by supramolecular interactions in the ligand backbone (b).

Table 1.1 Catalyst library through mixing of *n* monodentate ligands.

Ligand	$\mathbf{L^1}$	$\mathbf{L^2}$	⋯	$\mathbf{L^n}$
L^1	$L^1\,L^1$			
L^2	$L^1\,L^2$	$L^2\,L^2$		
⋯	⋯	⋯	⋯	
L^n	$L^1\,L^n$	$L^2\,L^1$	⋯	$L^n\,L^n$

ligand metal complexes will be obtained. This results in three potential catalysts present in solution (Scheme 1.2a). Only when the heterocombination is more active and selective than both homocombinations, a better catalyst could be obtained by optimization.

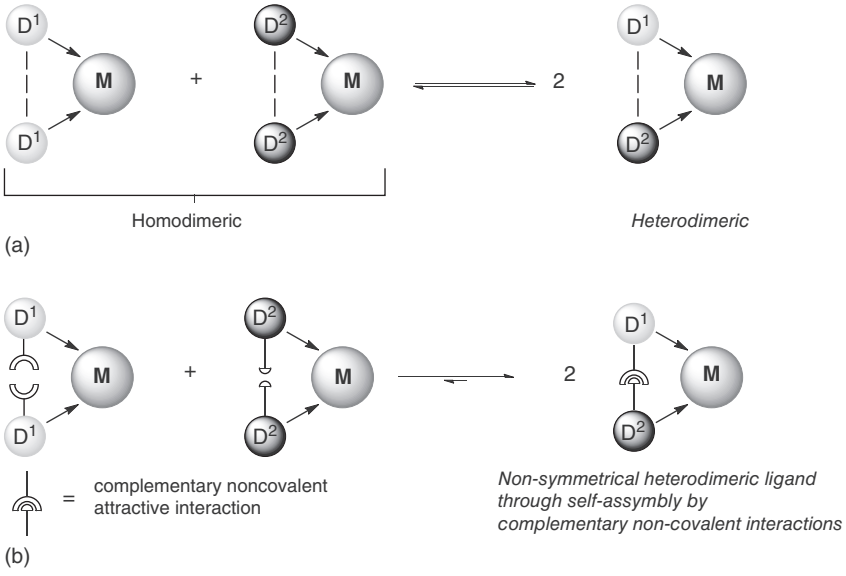

Scheme 1.2 Catalytic mixtures of two ligands D^1 and D^2 and a metal source when the ligands have noncomplementary D^1/D^2 interactions (a). Catalytic mixture of monodentate ligands with complementary binding sides in the presence of a metal source leads to single defined heterodimeric catalysts (b).

Table 1.2 Catalyst library with $m \times n$ different and defined heterodimeric ligand combinations obtained by the mixing of two sets of monodentate ligands with complementary binding sites.

Ligand	m_1	m_2	⋯	m_i
n_1	m_1n_1	m_2n_1	⋯	m_in_1
n_2	m_1n_2	m_2n_2	⋯	m_in_2
⋯	⋯	⋯	⋯	⋯
n_j	m_1n_j	m_2n_j	⋯	m_in_j

For achieving reasonable understanding in the construction of a ligand library, it is desirable that only the heterodimeric combinations are preferably formed. This problem could be solved using two sets of monodentate ligands with complementary binding sides, which enables only attractive ligand–ligand interactions in case of the heterodimeric combination (Scheme 1.2b).

Such a heterodimeric ligand system formed by complementary self-assembly could imitate classical nonsymmetrical ligand systems. If now m ligands of the set D^1 and n ligands of the set D^2 are mixed in the presence of a transition metal species, a library of $m \times n$ defined heterodimeric bidentate ligand–metal complexes is formed (Table 1.2).

In this chapter, we will focus on the results of our own research group on hydrogen bonding to construct self-assembling ligands. The concept is described and several applications in homogeneous catalysis are presented.

1.2 Formation of Bidentate Ligands Through Self-assembly via Hydrogen Bonding and Application in Hydroformylation

1.2.1 2-Hydroxypyridine/2-Pyridone Platform

In 2003, our group reported the *in situ* generation of bidentate ligands in the coordination sphere of a transition metal through self-assembly by hydrogen bonds [7]. This first example was based on the 2-pyridone (**1b**)/2-hydroxypyridine (**1a**) tautomers (Scheme 1.3). The parent system (D = H) dimerized in aprotic solvent predominantly as the symmetrical pyridone dimer **2**. However, when D is a donor group capable of coordinating a transition metal (e.g. PPh_2), it can be observed that in the presence of a transition metal, the equilibrium shifts toward the mixed hydroxypyridine/pyridone dimer **3**. This is reasonable, because only the mixture of the tautomers can benefit from the stabilization of both phosphines coordinating to the metal center and two hydrogen bonds.

In fact, for platinum and rhodium complexes of the 6-diphenylphosphanyl-2-pyridone (6-DPPon) ligand **1**, the self-assembly by hydrogen bonding could be proven in solution using NMR and in solid state by X-ray crystal structure analysis (Figure 1.1) [7, 8].

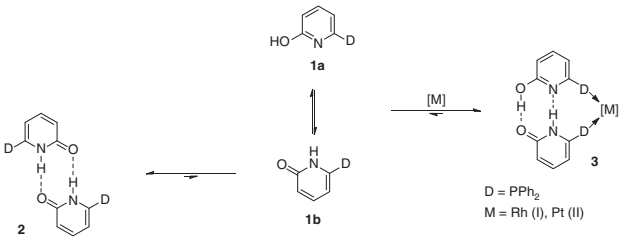

Scheme 1.3 Self-assembly of the pyridone system and in the presence of a metal source self-assembly of the 2-pyridone/2-hydroxypyridine to form bidentate complexes **3** suitable for homogeneous catalysis.

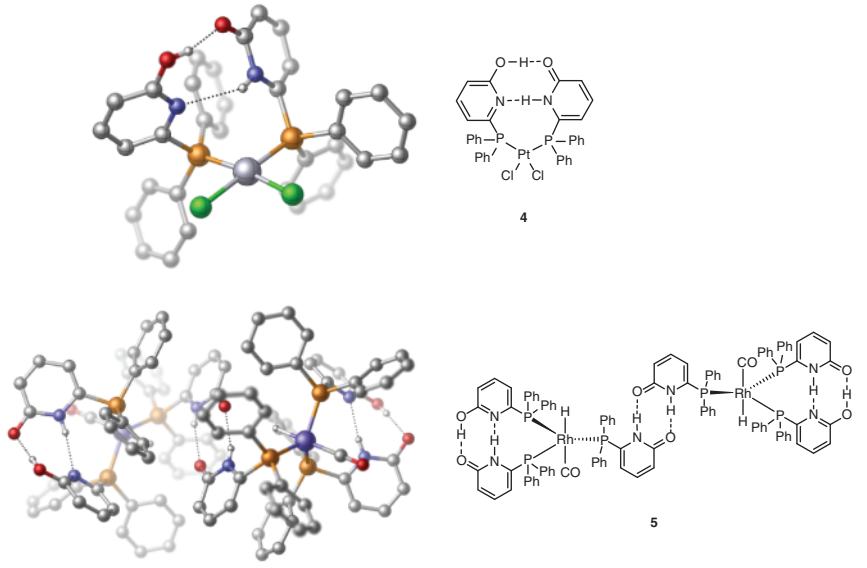

Figure 1.1 X-ray structure of a $[Cl_2Pt(6\text{-DPPon})_2]$-complex [7] (**4**) and a dimer of a $[HRh(6\text{-DPPon})_3(CO)]$-complex (**5**) (carbon-bonded hydrogen atoms are omitted for clarity) [8].

In rhodium-catalyzed hydroformylation of terminal alkenes, a catalyst based on the 6-DPPon ligand showed high selectivities for the linear aldehyde, which are typical of classical bidentate ligands [7]. However, bidentate ligands usually have lower catalytic activity compared with unselective monodentate ligands [9]. Therefore, the 6-DPPon ligand combines the advantages of mono- and bidentate ligands. This catalytic system tolerates many functional groups in the alkene substrate (Table 1.3). Among the tested substrates, some are even capable of forming hydrogen bonds such as carbamates, salicylates, or even free alcohols. If the hydrogen bonds of the ligand system are disrupted, the selectivities of the catalyst drop significantly. Potential sources for disruption are high temperatures above 110 °C, protic solvents, or acidic conditions (Table 1.3, entry 9 and 10).

Table 1.3 Regioselective rhodium-catalyzed hydroformylation of terminal alkenes with the 6-DPPon ligand.[a)]

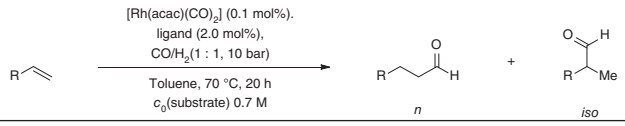

#	Substrate	n:iso 6-DPPon	n:iso PPh_3	#	Substrate	n:iso 6-DPPon	n:iso PPh_3
1	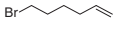	97 : 3	72 : 28	6	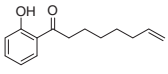	95 : 5	70 : 30
2	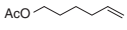	96 : 4	71 : 29	7		95 : 5	89 : 11
3	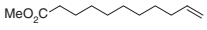	97 : 3	74 : 26	8		96 : 4	77 : 23
4	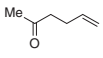	94 : 6	71 : 29	9[b)]		83 : 17	77 : 23
5	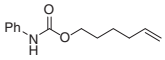	96 : 4	69 : 31	10[c)]		81 : 19	—

a) Reaction conditions: $[Rh(acac)(CO)_2]$/ligand/substrate = 1 : 20 : 1000, c_0(substrate) = 0.7 M, toluene, CO/H_2 (1 : 1, 10 bar), 70 °C. Full conversion was reached in every case after 20 hours.
b) MeOH as solvent.
c) Addition of 0.5 equiv of AcOH with respect to substrate.

The extraordinary importance of hydrogen bonding for the high activity and selectivity in rhodium-catalyzed hydroformylation was shown by detailed NMR and *in situ* IR spectroscopical investigations, ESI-MS as well as by DFT calculations [8, 10–13]. The hydrogen bonding in the ligand backbone seems to provide a flexibility that enables an easy change of coordination geometries without significant energy penalty, while on the other hand, they provide the structural stability to obtain high selectivities for the linear product.

The high activity of catalysts based on the 6-DPPon ligand in rhodium-catalyzed hydroformylation was highlighted in the first room-temperature ambient-pressure hydroformylation of terminal alkenes [14]. Using only low catalysts loading, a wide range of alkenes could be transformed into the related aldehydes in high yield and excellent selectivity (Table 1.4). In further studies of this approach, even water could be employed as a solvent, when a small amount of a specific surfactant was added [15]. This protocol is highly attractive for application in organic chemistry, because no special high-pressure equipment is necessary and the products are easily obtained in high yields and selectivity.

Although hydroformylation of terminal alkenes is a well-established transformation in homogeneous catalysis, alkynes or allenes are way less used as substrates in hydroformylation, not just because of the usual low chemo- and regioselectivity (Scheme 1.4), but also in general low activity of these substrates. However, the hydroformylation of alkynes, for example, would offer an elegant atom-economic

Table 1.4 Room-temperature/ambient-pressure regioselective hydroformylation of terminal alkenes.

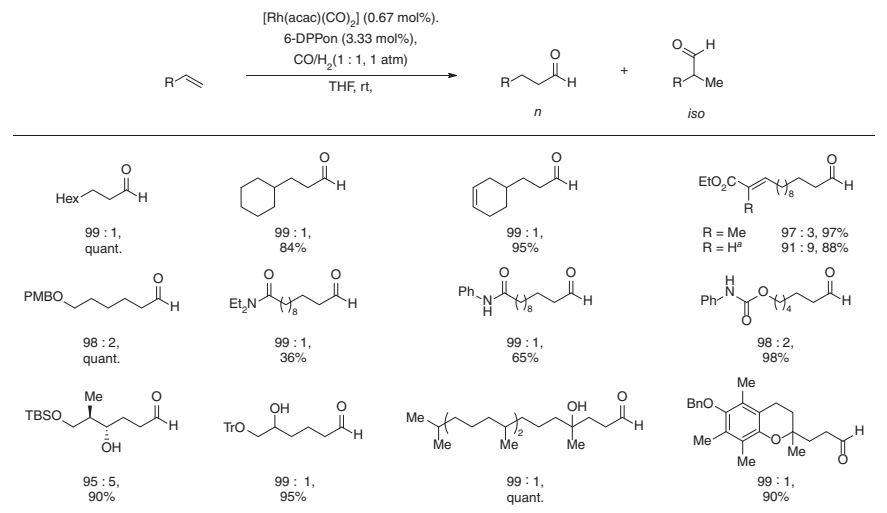

[a]Internal double bond is hydrogenated over time.

a) Internal double bond is hydrogenated over time.

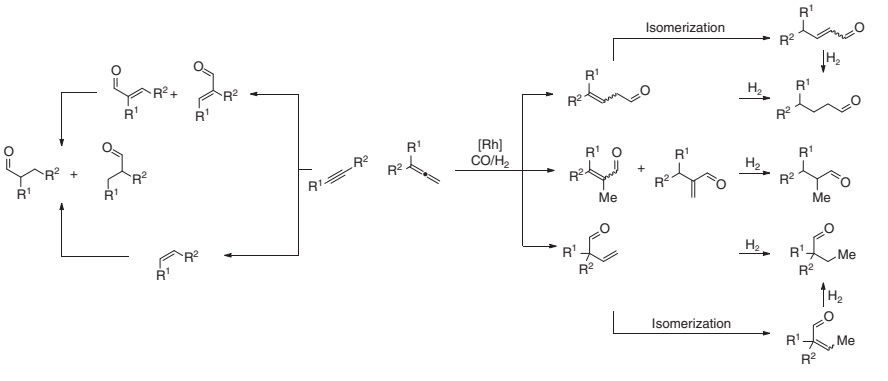

Scheme 1.4 Potential products in alkyne and allene hydroformylation.

way for the direct synthesis of enals. Major side products are the alkene and the saturated aldehydes, which are formed by either hydrogenation of the enals or hydroformylation of the alkene.

Using an electron poor derivative **6** of the 6-DPPon ligand, a huge range of internal alkynes could be used as substrate for this reaction to generate enals in high yield and excellent chemoselectivity (Scheme 1.5) [16]. Terminal alkynes were found to be a more challenging substrate, because the produced enals undergo easily hydrogenation of the conjugated double bond. Nevertheless, it was possible to generate three different enals in moderate yields, whereby a significant substrate influence on the selectivity was observed.

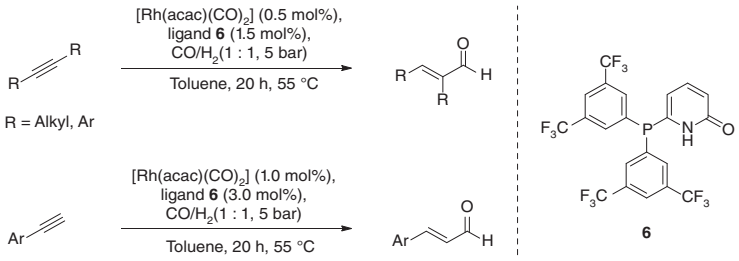

Scheme 1.5 Hydroformylation of internal and terminal alkynes.

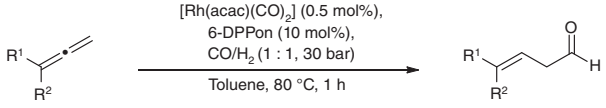

Scheme 1.6 Synthesis of γ,β-unsaturated aldehydes by allene hydroformylation.

The 6-DPPon ligand was also able to convert several 1,1-disubstituted allenes into γ,β-unsaturated aldehydes (Scheme 1.6) [17]. These unusual building blocks were obtained in high regio- and chemoselectivity. When unsymmetrically 1,1-disubstituted allenes were used as substrates, the *Z*-product was formed in up to >95% selectivity. The achieved yield was usually very high, and the catalyst can be used to synthesize the products even in gram scale. The allenes required for this protocol can be readily prepared in a simple two-step synthesis from almost any ketone [17].

1.2.2 Complementary Hydrogen Bonding for the Construction of Heterodimeric Self-assembling Ligands

The tautomers of 6-DPPon ligand **1** are indistinguishable in transition metal complexes due to a fast equilibration process [10]. This behavior is not beneficial if two pyridone ligands with different donor sites are mixed together, because mixtures of the two homodimeric and the heterodimeric complex would be obtained (Scheme 1.2). For the synthesis of a pure heterodimeric catalyst, another concept must be applied: complementary self-assembly. Inspired by the A–T base pairing of DNA, a complementary platform based on aminopyridine and isoquinolone was tailored (Scheme 1.7) to enable exclusively the synthesis of heterodimeric self-assembled ligand complexes [18].

The phosphine ligands **7** and **8** based on this platform (D = PPh_2) form in the presence of [Cl_2Pt(COD)] exclusively the heterodimeric *cis*-[Cl_2Pt(**7**)(**8**)] complex **10**. The complementary self-assembly of both ligands by hydrogen bonding was found in solid-state by X-ray crystal structure analysis (Figure 1.2) and in solution by a low field shift of the involved protons in the ^{1}H-NMR.

These platforms allow the selective formation of ligand libraries based on hydrogen bonding by variation of the donor group of one or both ligands (Table 1.2). Applying this concept, it was possible to identify a catalyst with outstanding activity and high regioselectivity in the rhodium-catalyzed hydroformylation of 1-octene

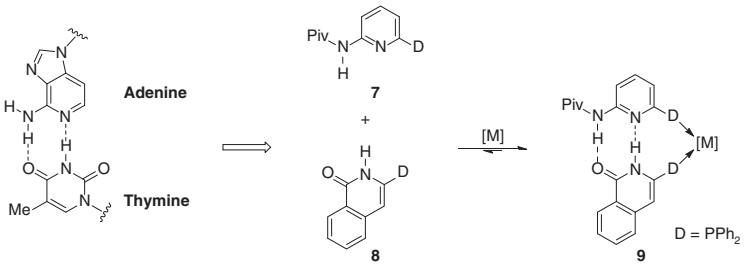

Scheme 1.7 An A–T-base pair as a model for a complementary self-assembly ligand platform via hydrogen bonds.

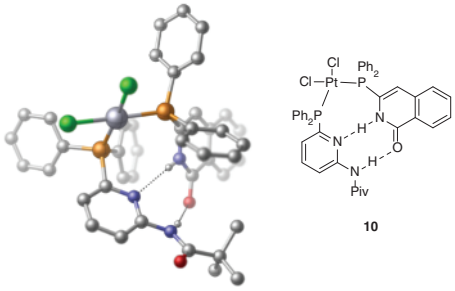

Figure 1.2 X-ray crystal structure of a [Cl_2Pt(**7a**)(**8a**)]-complex **10** (carbon-bonded hydrogen atoms are omitted for clarity) [18].

(Table 1.5) [18]. It should be highlighted that it is a nonsymmetrical combination of donor groups of the ligands.

The complementary self-assembly approach is not restricted to the aminopyridine/isoquinolone system only. The A–T base pair analogous platform could be modified as well [19]. Any modifications on this part of the ligand might affect directly the hydrogen bonding system and by that directly to ligand bite angle and coordination geometry to a metal. These parameters have a significant influence of the performance of a catalyst. In this sense, several ligands with modified hydrogen bonding systems were synthesized and explored (Scheme 1.8) [19].

Of all 10 ligand combinations [Cl_2Pt(L^{DA})(L^{AD})], complexes were prepared and studied. By ^{1}H and ^{31}P NMR spectroscopy, it was possible to show that all combinations form in solution selectively heteroleptic *cis*-complexes with hydrogen bonds. By X-ray crystal structure analysis, the defined structure could furthermore be confirmed for the solid state for the complexes of [Cl_2Pt(**13**)(**8a**)] and [Cl_2Pt(**12**)(**15**)] (Figure 1.3).

To evaluate the catalytic potential of these ligands, they were tested independently in the rhodium-catalyzed hydroformylation of 1-octene [19]. The obtained regioselectivities of all ligands were in a typical order of monodentate ligands such as PPh_3 (from 75 : 25 to 81 : 19). Afterward all 10 ligand combinations were tested under the same conditions (Table 1.6). The observed regioselectivities (89 : 11 to >99 : 1) indicate that in all cases the bidentate self-assembled ligand might be the kinetically competent catalyst.

Table 1.5 Turnover frequencies and regioselectivities for a 4 × 4 ligand matrix of aminopyridine (**7a–d**) and isoquinolone (**8a–d**) derived self-assembled bidentate ligands in the rhodium-catalyzed hydroformylation of 1-octene.

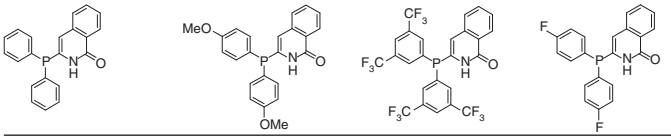

Ligand	8a	8b	8c	8d
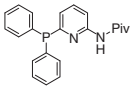 **7a**	2425 h^{-1} 94 : 6	1040 h^{-1} 94 : 6	2732 h^{-1} 96 : 4	2559 h^{-1} 95 : 5
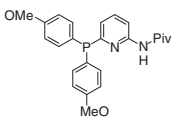 **7b**	2033 h^{-1} 93 : 7	1058 h^{-1} 92 : 8	1281 h^{-1} 96 : 4	1772 h^{-1} 94 : 6
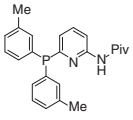 **7c**	3537 h^{-1} 94 : 6	1842 h^{-1} 93 : 7	1808 h^{-1} 96 : 4	2287 h^{-1} 94 : 6
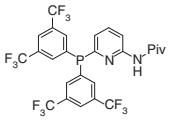 **7d**	7439 h^{-1} 96 : 4	2695 h^{-1} 95 : 5	7465 h^{-1} 94 : 6	**8643 h^{-1}** **96 : 4**

Reaction conditions: $[Rh(acac)(CO)_2] : L^{AD} : L^{DA}$: 1-octene = 1 : 10 : 10 : 7500, CO/H_2 (1 : 1, 10 bar), toluene, c_0(1-octene) = 2.91 M, 5 hours. Catalyst preformation: CO/H_2 (1 : 1, 5 bar), 30 minutes, rt to 80 °C.

Remarkably, the combinations in which the pivaloyl group of the ligands **7a** and **13** was substituted by a trifluoroacetyl group, an increase in regioselectivity was observed. This might be related to an increased strength in hydrogen bonding. Of all studied ligand combinations, the catalyst formed from **14**/**8a** and **14**/**15** showed the highest selectivity (Table 1.7). A regioselectivity for the linear aldehyde of more than 99:1 was achieved. One explanation for this improvement might be that by the change of the ring size of the six-membered aminopyridine system to the five-membered thiazole heterocycle, the accessible geometry of the system

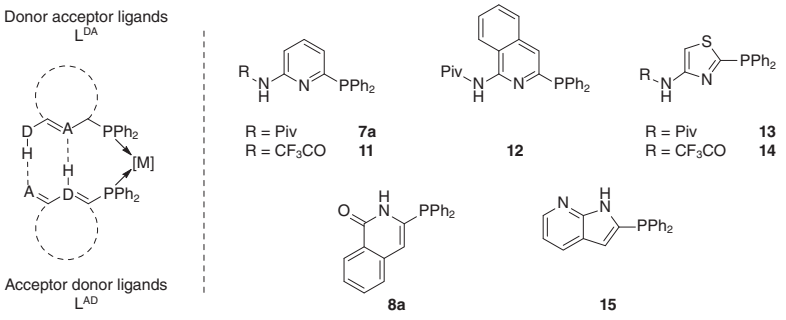

Scheme 1.8 Library of ligands with complementary hydrogen bonding platform.

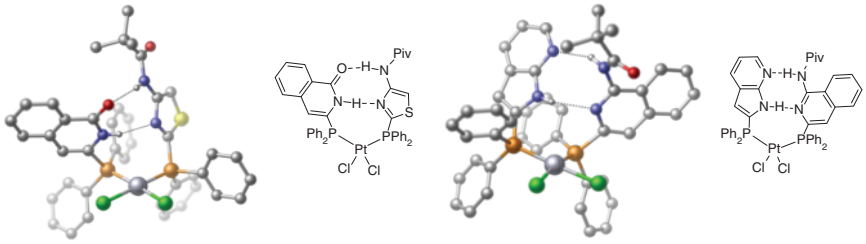

Figure 1.3 X-ray crystal structure of a [Cl_2Pt(**13**)(**8a**)]- and a [Cl_2Pt(**12**)(**15**)]-complex (carbon-bonded hydrogen atoms are omitted for clarity).

Table 1.6 Turnover frequencies and regioselectivities for a 5 × 2 ligand matrix with different combinations of DA- and AD-ligands as self-assembled bidentate ligands in the rhodium-catalyzed hydroformylation of 1-octene.

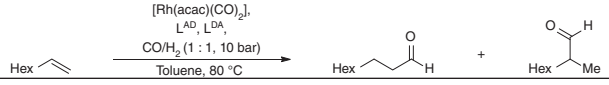

Ligand	7a	11	12	13	14
8a	2394 h^{-1} (93 : 7)	3396 h^{-1} (96 : 4)	2452 h^{-1} (95 : 5)	3890 h^{-1} (98 : 2)	3888 h^{-1} (**>99 : 1**)
15	2679 h^{-1} (89 : 11)	4864 h^{-1} (96 : 4)	3205 h^{-1} (95 : 5)	3233 h^{-1} (95 : 5)	2333 h^{-1} (**99 : 1**)

Reaction conditions: [Rh(acac)$(CO)_2$] : L^{AD} : L^{DA} : 1-octene = 1 : 10 : 10 : 7500, CO/H_2 (1:1, 10 bar), toluene, 80 °C, 5 hours. Catalyst preformation: CO/H_2 (1 : 1, 5 bar), 30 minutes, rt to 80 °C.

Table 1.7 Regioselectivities of the rhodium-catalyzed hydroformylation of 1-octene in toluene or MeOH as solvent.

#	Ligands	*l* : *b* in toluene	*l* : *b* in MeOH
1	**7a**/**8a**	94 : 6	82 : 18
2	**11**/**8a**	96 : 4	79 : 21
3	**13**/**8a**	98 : 2	97 : 3
4	**14**/**8a**	99 : 1	96 : 4

Reaction conditions: $[Rh(acac)(CO)_2]$, [Rh] : L^{AD} : B1 : 1-octene = 1 : 10 : 10 : 7500, CO/H_2 (1:1, 10 bar), 80 °C; Regioselectivity: linear to branched, determined by GC-analysis and/or ^1H NMR spectroscopy.

is slightly changed. By this, more stable hydrogen bonds seem to be formed, which might yield a more rigid system. If this assumption is correct, it should be interesting to test these ligands in protic solvents such as methanol. First generation of self-assembly ligands such as 6-DPPon or **7a**/**8a** showed a significant drop of the regioselectivity in the hydroformylation of 1-octene in protic solvents [7, 18]. This sensitivity to protic solvents so far limits the application range of self-assembled ligands in homogeneous catalysis.

Therefore several ligand combinations were studied in the rhodium-catalyzed hydroformylation of 1-octene in methanol and toluene. The combinations without the thiazole-based ligands suffered a significant loss of regioselectivity in methanol. This drop in selectivity indicates a disruption of the hydrogen bonds in the backbones of these ligands, which leads to results similar to a catalyst based on PPh_3. Combinations that involve a thiazole ligand result in high regioselectivity in both toluene and methanol.

These findings clearly show that the variation of the heterocyclic platform for the hydrogen bonds has a huge influence on the resulting catalyst. Thus, new catalysts for the rhodium-catalyzed hydroformylation could be identified with a very high activity and an almost perfect regioselectivity. These catalysts could successfully be applied in protic solvents, which is a huge step for the applicability of self-assembled ligands based on hydrogen bonding.

1.3 Asymmetric Hydrogenation

1.3.1 P-chiral Self-assembly Ligands in Asymmetric Hydrogenation

To study the power of the combinatorial approach in asymmetric catalysis, a library of new chiral ligands was synthesized [20, 21], carrying the previously established platforms for complementary self-assembly via hydrogen bonding (Scheme 1.9).

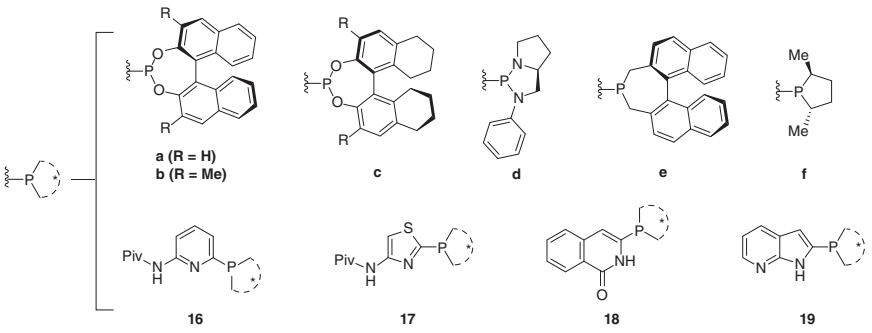

Scheme 1.9 Library of chiral self-assembly ligands.

In total, 12 AD-ligands and 10 DA ligands were prepared and tested in the asymmetric rhodium-catalyzed hydrogenation by mixing all possible ligand combinations [21]. In total, 120 catalysts are possible due to the complementary hydrogen bonding. These catalysts were investigated and seven combinations showed perfect ee and high or quantitative conversion (Table 1.8). The disadvantage of this approach is the high number of experiments to identify all promising ligand combinations.

One elegant way to overcome this drawback is a combinatorial approach using an iterative deconvolution strategy (Table 1.9). First step of this strategy is the division of all ligands of this ligand library into subgroups. Each subgroup is mixed with the corresponding other subgroups. The results of all subgroup combinations are compared and the best combination in terms of selectivity and activity is further deconvoluted by division into new subgroups. All other combinations are discarded and the process will be repeated until the most active and selective catalyst is identified. By this methodology three individual catalysts with perfect activity and enantioselectivity could be identified in only 17 reactions instead of 120 of the classical approach. This strategy not only reduces the number of reactions to be run dramatically, but also the analytical effort is reduced to the same extent.

1.3.2 Inducing Axial Chirality in a Supramolecular Catalyst

Ligands with an axial chiral backbone are among the most valuable systems used in asymmetric catalysis [22–25], but the synthesis of their inflexible backbone is often long and difficult. Recently, a new type of *in silico* designed ligand was presented [26]. This ligand is based on the 6-DPPon ligand, but carries a chiral substituent at the pyridone ring (Scheme 1.10). In transition metal complexes, this ligand self-assembles by hydrogen bonding of its tautomeric forms. However, the so formed supramolecular backbone is twisted and axially chiral, which results in two diastereomeric complexes. Rhodium and platinum complexes of these ligands were studied by ESI-MS, NMR-, UV-, and circular dichroism spectroscopy. The ratio of these complexes in solution is very sensitive to temperature and solvent effects.

Table 1.8 Parallel screening of a library of 120 self-assembled catalysts in the rhodium-catalyzed asymmetric hydrogenation by the classic approach.

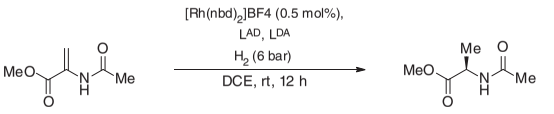

L^{DA}	L^{AD}	(*S*)-**17a**	(*S*)-**17b**	(*S*)-**17c**	(*S*)-**17d**	(*S*)-**17e**	(*S*)-**17f**	(*S*)-**16a**	(*S*)-**16b**	(*S*)-**16c**	(*S*)-**16d**	(*S*)-**16e**	(*S*)-**16f**
		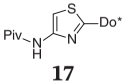 **17**						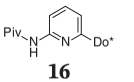 **16**					
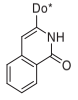 **18**	(*S*)-**18a**	**99 (quant.)**	96 (quant.)	95 (quant.)	88 (quant.)	**99 (quant.)**	79 (quant.)	**99 (86)**	97 (88)	96 (89)	89 (quant.)	**99 (90)**	81 (93)
	(*S*)-**18b**	90 (quant.)	91 (99)	90 (98)	92 (quant.)	90 (quant.)	84 (quant.)	92 (84)	89 (86)	91 (85)	86 (89)	93 (86)	85 (94)
	(*S*)-**18c**	94 (quant.)	82 (98)	88 (97)	90 (quant.)	95 (quant.)	88 (quant.)	94 (83)	93 (79)	87 (78)	88 (81)	90 (84)	81 (85)
	(*S*)-**18d**	92 (quant.)	88 (quant.)	81 (quant.)	66 (quant.)	91 (quant.)	60 (quant.)	89 (quant.)	84 (98)	85 (95)	54 (90)	88 (quant.)	40 (88)
	(*S*)-**18e**	**99 (quant.)**	94 (quant.)	92 (quant.)	89 (quant.)	98 (quant.)	90 (quant.)	**99 (89)**	98 (87)	94 (86)	84 (95)	**99 (92)**	79 (95)
	(*S*)-**18f**	87 (quant.)	89 (quant.)	90 (quant.)	80 (quant.)	88 (quant.)	78 (quant.)	93 (quant.)	95 (95)	94 (89)	81 (95)	89 (87)	74 (83)
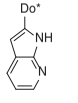 **19**	(*S*)-**19a**	90 (quant.)	87 (94)	90 (92)	41 (96)	91 (quant.)	76 (53)	88 (85)	87 (78)	91 (81)	46 (84)	87 (90)	79 (47)
	(*S*)-**19b**	82 (quant.)	77 (72)	85 (57)	49 (80)	81 (quant.)	39 (15)	84 (81)	83 (80)	89 (59)	55 (73)	85 (81)	48 (58)
	(*S*)-**19c**	78 (quant.)	66 (89)	74 (35)	37 (77)	79 (quant.)	36 (14)	80 (82)	71 (71)	77 (65)	49 (68)	82 (85)	20 (64)
	(*S*)-**19d**	81 (quant.)	81 (84)	84 (66)	52 (98)	82 (quant.)	43 (56)	83 (88)	82 (58)	86 (67)	38 (quant.)	80 (87)	44 (78)

Reaction conditions: $[Rh(nbd)_2]BF_4$, [Rh] : L^{AD} : L^{DA} : substrate = 1 : 1.05 : 1.05 : 200, H_2 (6 bar), DCE, c_0(substrate) = 0.3 M, 12 hours, RT. Enantioselectivity was determined by chiral GC, conversion was determined by ^{1}H NMR spectroscopy.

ee

(conv.)

Table 1.9 Combinational approach to the identification of the most active and selective ligand combinations in the rhodium-catalyzed asymmetric hydrogenation.

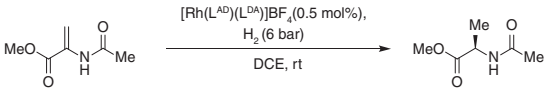

Step 1	L^{AD}	17	16
L^{DA}	Do	(*S*)-**17a** (*S*)-**17b** (*S*)-**17c** (*S*)-**17c** (*S*)-**17e** (*S*)-**17f**	(*S*)-**16a** (*S*)-**16b** (*S*)-**16c** (*S*)-**16c** (*S*)-**16e** (*S*)-**16f**
18	(*S*)-**18a** (*S*)-**18b** (*S*)-**18c** (*S*)-**18d** (*S*)-**18e** (*S*)-**18f**	84% *ee* (quant.)	79% *ee* (quant.)
19	(*S*)-**19a** (*S*)-**19b** (*S*)-**19c** (*S*)-**19d**	62% *ee* (92%)	

Step 2		17		
L^{DA}	Do	(*S*)-**17a** (*S*)-**17e**	(*S*)-**17b** (*S*)-**17d**	(*S*)-**17c** (*S*)-**17f**
18	(*S*)-**18a** (*S*)-**18e**	99% *ee*	93% *ee*	87% *ee*
	(*S*)-**18b** (*S*)-**18c**	92% *ee*	89% *ee*	89% *ee*
	(*S*)-**18d** (*S*)-**18f**	82% *ee*	84% *ee*	84% *ee*

Step 3		17	
L^{DA}	Do	(*S*)-**17a**	(*S*)-**17e**
18	(*S*)-**18a**	99% *ee*	99% *ee*
	(*S*)-**18e**	99% *ee*	98% *ee*

Reaction conditions: $[Rh(nbd)_2]BF_4$, [Rh] : L^{AD} : L^{DA} : substrate = 1 : 1.05 : 1.05 : 200, H_2 (6 bar), DCE, c_0(substrate) = 0.3 M, 12 hours, RT. Enantioselectivity was determined by chiral GC, conversion was determined by ^{1}H NMR spectroscopy.
The shades should highlight the conditions which gave the highest yield and enantioselectivity.

At room temperature, both diastereomeric complexes are indistinguishable, but at lower temperatures, one complex is favored.

The potential of this concept was shown in rhodium-catalyzed asymmetric hydrogenation. With the ligands **20S** and **20R,** enantiomeric excess up to 90% could be achieved (Table 1.10). Control experiments in MeOH showed how crucial hydrogen bonding is to achieve enantioselectivity.

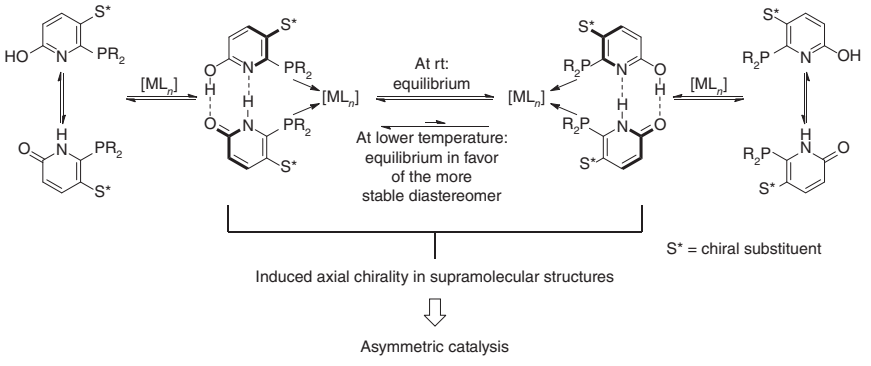

Scheme 1.10 Induced axial chirality in supramolecular structures.

Table 1.10 Asymmetric hydrogenation of methyl acetamidoacrylate.

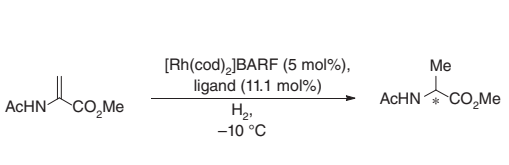

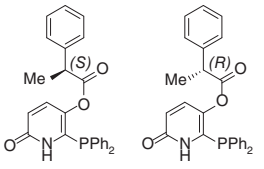

20S **20R**

#	Ligand	Solvent	Conversion (%)	*ee* (%)
1	**20S**	DCE	85	84 (*S*)
2	**20R**	DCE	81	85(*R*)
3	**20S**	*o*-DCB	93	90 (*S*)
4	**20S**	MeOH	1	*rac*.

[Rh]/L/substrate 1 : 2.2 : 20; *c*(substrate) = 0.02 M; conversion and ee determined by chiral-phase GC. BARF = *tetrakis*[3,5-*bis*(trifluoromethyl)phenyl]borate.

1.4 Other Catalytic Applications

Self-assembling ligands are not limited to rhodium-catalyzed hydroformylation or hydrogenation reactions. This methodology was successfully applied on several reactions.

1.4.1 Hydration of Alkynes

The addition of water to alkynes is an important way to install functional groups into a carbon skeleton. This transformation usually follows the Markovnikov rule [27–31]. An *anti*-Markovnikov selective hydration of a terminal alkyne would be a convenient method to generate aldehydes. For this unusual hydration mode, only few ruthenium catalysts were previously reported [32–37]. Bidentate ligands [35],

phosphinopyridine ligands [34], and the preorientation of the water molecule by hydrogen bonding [33] seemed to have positive effects in the reported processes. Self-assembling ligands also incorporate a pyridinyl-functionalized phosphine group, and they emulate bidentate ligands with their hydrogen bonding system, which might interact with water.

To obtain further insight, the hydration of 1-nonyne catalyzed by half-sandwich ruthenium complexes with different ligands was investigated [38]. With mono- or bidentate phosphine ligands, only low activity and selectivity were observed (Table 1.11, entries 1–3). The 6-DPPon ligand, which should be able to self-assemble by hydrogen bonding, showed similar results (entry 4). However, a catalyst based on the complementary self-assembling of the heterodimeric aminopyridine/isoquinolone ligands yielded the desired product in perfect selectivity with excellent catalyst activity (entry 5). By control experiments, it was shown that the heterodimeric ligand combination is responsible for the best catalyst (entries 6 and 7).

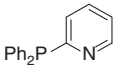

dppy

dppe

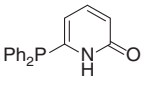

6-DPPon

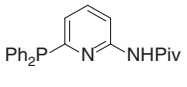

7a

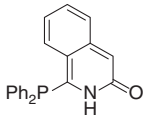

8a

Table 1.11 Ruthenium complex-catalyzed hydration of 1-nonyne.

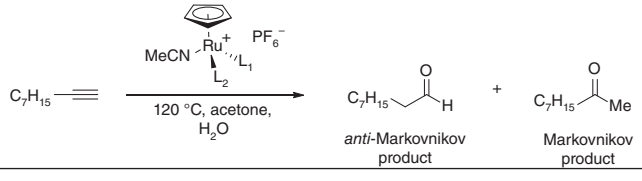

#	Cat.	L1	L2	*t* (h)	Aldehyde[a] (%)	Ketone[a] (%)
1		PPh_3	PPh_3	140	1.2	18
2[b]		dppy	dppy	168	4.0	2.4
3		dppe	—	168	2.1	20
4[b]		6-DPPon (**1**)	6-DPPon(**1**)	168	2.1	25
5		(**7a**)	(**8a**)	26	94	0
6[b]		(**7a**)	(**7a**)	72	39	3.8
7		(**8a**)	(**8a**)	48	1.9	0

a) Yield calculated from GC response factors relative to internal standard hexadecane.
b) κ^1-P, κ^2-P,N coordination of the phosphinopyridine with replacement of the acetonitrile ligand.

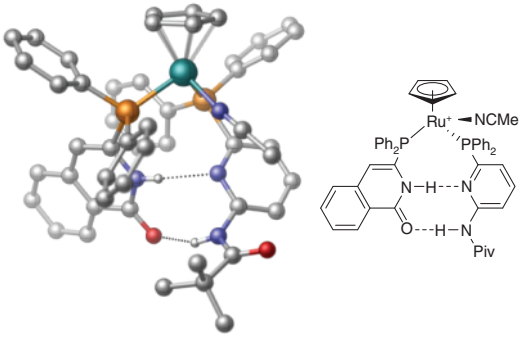

Figure 1.4 X-ray crystal structure of a [(Cp)Ru(**7a**)(**8a**)(NCMe)]$^{+}$-complex (carbon-bonded hydrogen atoms and the PF_6^- counterion are omitted for clarity.

The structure of the best catalyst was further analyzed by X-ray crystal structure analysis and the hydrogen bonding was confirmed (Figure 1.4). This catalyst was applied on a scope of 10 different alkynes with in almost all cases perfect chemoselectivity for the aldehyde and good-to-excellent activities.

1.4.2 Hydration of Nitriles

Classical hydration of nitriles to amides requires very harsh conditions [39]. Transition metal catalysis offers a powerful tool to perform this reaction under very mild conditions [40, 41]. For this reason, the hydration of nitriles to amides is an important example of an industrially important atom economic reaction [42]. After the successful application of the self-assembly ligands in the hydration of alkynes, it seemed promising to apply these ligands also to nitriles. For this reason, homo- and heterodimeric *bis*(acetylacetonato)ruthenium(II) complexes of the ligands **7a** and **8a** were prepared [43]. The structure of these complexes was investigated in solution and in solid state. Especially for the heterodimeric combination, some unusual hydrogen bonding patterns were observed involving hydrogen bonding in between the **8a** ligand and an oxygen atom of an acac ligand (Figure 1.5).

However, the homo-complex of **8a** showed the highest activity in the hydration of *p*-tolylcarbonitrile (Table 1.12).

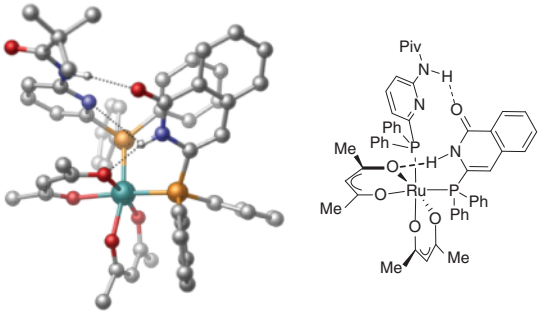

Figure 1.5 X-ray crystal structure of a [Ru(acac)$_2$(**7a**)(**8a**)]-complex (carbon-bonded hydrogen atoms are omitted for clarity) [43].

Table 1.12 Ruthenium complex-catalyzed hydration of nitriles.

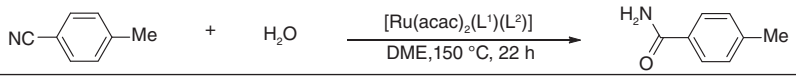

#	L^1	L^2	Conversion (%)	TOF (h^{-1})
1	**8a**	**8a**	100	20
2	**8a**	**7a**	90	5
3	**7a**	**7a**	<5	nd

Reaction conditions: $[Ru(acac)_2(L^1)(L^2)]$/substrate/water = 1 : 100 : 200, DME (1 ml), substrate (1 mmol), water (2 mmol), 150 °C, 22 hours.

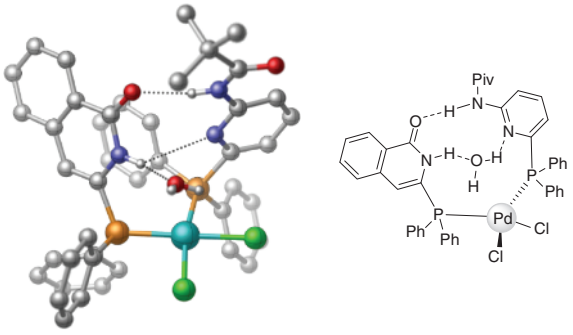

Figure 1.6 X-ray crystal structure of $[Cl_2Pd(\mathbf{8a}\cdot H_2O)(\mathbf{7a})]$ (carbon-bonded hydrogen atoms are omitted for clarity) [44].

1.4.3 Allylic Substitution with Allylic Alcohols

It was possible to synthesize crystals of a $[Cl_2Pd(\mathbf{8a}\cdot H_2O)(\mathbf{7a})]$ suitable for X-ray structure analysis (Figure 1.6) [44]. Interestingly, a single water molecule was incorporated in the hydrogen bonding system of the complementary self-assembly ligands.

Inspired by this interaction of water with the ligand backbone, it seemed reasonable that alcohols might form similar interactions [44]. Especially allylic alcohols might be directed by this interaction in a beneficial orientation with the palladium center. Indeed, it was possible to apply directly allylic alcohols as substrates in allylic substitution with water as the only by-product (Scheme 1.11). The common substrates of classic allylic substitution catalysts are in most cases allylic acetates or carbonates [45]. These substrates have to be prepared in an extra step and release always a stoichiometric amount of a coupled byproduct. The palladium-catalyzed allylic substitution with the self-assembly ligands can directly apply allylic alcohols and generates as stoichiometric by-product only water.

1.4.4 Hydrocyanation

The nitrile group is often found in many natural products as well as in different pharmaceuticals, agrochemical products, and functional materials [46]. The nitrile

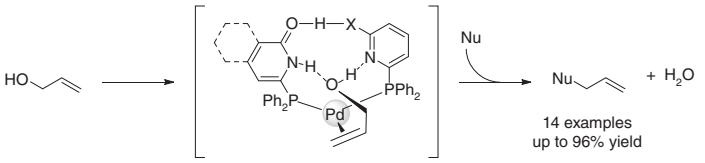

Scheme 1.11 Palladium complex-catalyzed allylic substitution of allylic alcohols directed by substrate pre-orientation through hydrogen bonding to self-assembled ligands.

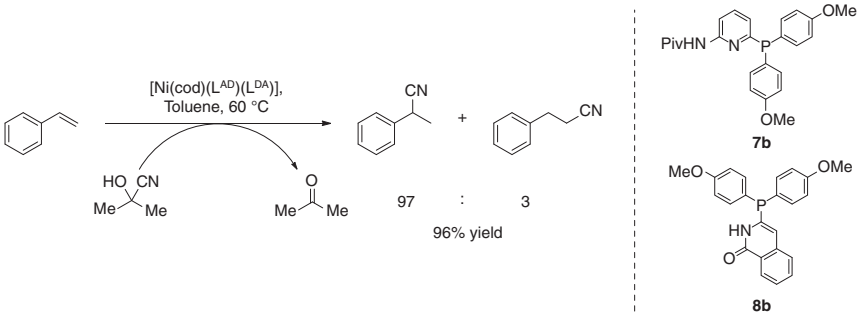

Scheme 1.12 Nickel complex-catalyzed hydrocyanation of alkenes.

group is also quite useful in organic synthesis because it can easily be transformed into different functional groups such as amines, aldehydes, ketones, and other carboxylic acid derivatives [47]. An elegant method to generate these molecules is the hydrocyanation of alkenes by the formal addition of HCN to a C=C double bond [48, 49]. Most industrial catalysts are based on (bidentate) phosphite or phosphinite ligands, but bidentate phosphine ligands showed also interesting reactivities [50]. Van Leeuwen et al. showed that electron poor bidentate ligands with bite angles around 105° seem to have positive results on the catalysts activity [51–53].

It has been demonstrated that the complementary heterodimeric self-assembly ligands can form Ni^0 complexes, which are promising catalysts in the hydrocyanation of styrenes [54]. A 5×4 ligand matrix of ligands derived from the isoquinolone and aminopyridine platform was used to identify the best ligand combination. The so found catalyst provided very high activity, perfect regioselectivity, and a good functional group tolerance in the nickel-catalyzed hydrocyanation of alkenes (Scheme 1.12). It is worth to highlight that the best ligand combination (**7b**/**8b**) bares electron-rich groups in contrast to previously reported catalysts, which seem to give better results with electron-poor ligands [52].

1.5 Concluding Remarks

In this chapter, the self-assembly of monodentate phosphine ligands in transition metal complexes by hydrogen bonding was described.

We have introduced the unique 6-DPPon ligand platform in homogeneous catalysis based on the homodimeric 2-pyridone/2-hydroxypyridine system. Catalysts

based on this platform showed an outstanding performance in rhodium-catalyzed hydroformylation of allenes, alkynes, and terminal alkenes, in some cases even at room temperature and under one atmosphere of syngas. Considering the limited accessibility of high-pressure equipment in many laboratories, this is a major advantage of this system. In addition, by introducing chiral substituents at the pyridone platform, an axial chiral self-assembled ligand system can be generated, which showed promising first results in asymmetric hydrogenation.

The A–T base pairing in the DNA inspired the complementary self-assembly of heterodimeric ligands. This approach offers easy access to the formation of structurally diverse ligand libraries. The huge advantage compared with classical bidentate ligands is that a catalyst composed of two unsymmetrical donors is easily realized just by mixing two complementary ligands together. For the synthesis of a comparable classic bidentate ligand with a covalent backbone and two unsymmetrical donor sites, a huge synthetic effort is necessary. Using these ligand libraries, it was possible to identify potent catalysts for many different transformations such as hydrocyanation, hydration of alkynes, or allylic substitution. Especially in rhodium-catalyzed hydroformylation, it was possible to generate outstanding active and selective catalysts. These catalysts enable perfect selectivity for the linear aldehyde even in protic solvents, which is an impressive proof for the stability of the supramolecular ligand backbone by hydrogen bonding. Nevertheless, large ligand libraries can still lead to a huge experimental effort to test all possible ligand combinations. In asymmetric hydrogenation, it was possible to give an example for the superiority of combinatorial methods to identify the most active catalyst, compared with the classical testing of all ligand combinations (17 instead of 120 reactions).

All those findings clearly show that the self-assembly of ligands by hydrogen bonding is a valuable tool for the synthetic chemist to use in homogeneous transition metal catalysis.

References

1 Hagen, J. (2015). Homogeneous catalysis with transition metal catalysts. In: *Industrial Catalysis: A Practical Approach*, 17–46. Weinheim, Germany: Wiley-VCH.

2 Hartwig, J.F. (2010). *Organotransition Metal Chemistry: From Bonding to Catalysis*. Mill Valley, California: University Science Books.

3 Schneider, H.-J. and Yatsimirsky, A.K. (2000). *Principles and Methods in Supramolecular Chemistry*. Chichester: Wiley.

4 Dydio, P. and Reek, J.N.H. (2014). Supramolecular control of selectivity in transition-metal catalysis through substrate preorganization. *Chem. Sci.* 5 (6): 2135–2145.

5 Lehn, J.-M. (1988). Supramolecular chemistry—scope and perspectives molecules, supermolecules, and molecular devices (nobel lecture). *Angew. Chem. Int. Ed. Engl.* 27 (1): 89–112.

6 Watson, J.D. and Crick, F.H. (1953). Molecular structure of nucleic acids; a structure for deoxyribose nucleic acid. *Nature* 171 (4356): 737–738.

7 Breit, B. and Seiche, W. (2003). Hydrogen bonding as a construction element for bidentate donor ligands in homogeneous catalysis: regioselective hydroformylation of terminal alkenes. *J. Am. Chem. Soc.* 125 (22): 6608–6609.

8 Gellrich, U., Seiche, W., Keller, M., and Breit, B. (2012). Mechanistic insights into a supramolecular self-assembling catalyst system: evidence for hydrogen bonding during rhodium-catalyzed hydroformylation. *Angew. Chem. Int. Ed. Engl.* 51 (44): 11033–11038.

9 Leeuwen, P.W.N.M. and Claver, C. (2002). *Rhodium Catalyzed Hydroformylation*. Dordrecht: Kluwer Academic Publishers.

10 Gellrich, U., Huang, J., Seiche, W. et al. (2011). Ligand self-assembling through complementary hydrogen-bonding in the coordination sphere of a transition metal center: the 6-diphenylphosphanylpyridin-2(1*H*)-one system. *J. Am. Chem. Soc.* 133 (4): 964–975.

11 Gellrich, U., Koslowski, T., and Breit, B. (2015). Full kinetic analysis of a rhodium-catalyzed hydroformylation: beyond the rate-limiting step picture. *Catal. Sci. Technol.* 5 (1): 129–133.

12 Gellrich, U., Himmel, D., Meuwly, M., and Breit, B. (2013). Realistic energy surfaces for real-world systems: an IMOMO CCSD(T):DFT scheme for rhodium-catalyzed hydroformylation with the 6-DPPon ligand. *Chemistry* 19 (48): 16272–16281.

13 Beierlein, C.H., Breit, B., Paz Schmidt, R.A., and Plattner, D.A. (2010). Online monitoring of hydroformylation intermediates by ESI-MS. *Organometallics* 29 (11): 2521–2532.

14 Seiche, W., Schuschkowski, A., and Breit, B. (2005). Bidentate Ligands by self-assembly through hydrogen bonding: a general room temperature/ambient pressure regioselective hydroformylation of terminal alkenes. *Adv. Syn. Catal.* 347 (11–13): 1488–1494.

15 Straub, A.T., Otto, M., Usui, I., and Breit, B. (2013). Room temperature ambient pressure (RTAP)-hydroformylation in water using a self-assembling ligand. *Adv. Syn. Catal.* 355 (10): 2071–2075.

16 Agabekov, V., Seiche, W., and Breit, B. (2013). Rhodium-catalyzed hydroformylation of alkynes employing a self-assembling ligand system. *Chem. Sci.* 4 (6): 2418.

17 Köpfer, A. and Breit, B. (2015). Rhodium-catalyzed hydroformylation of 1,1-disubstituted allenes employing the self-assembling 6-DPPon system. *Angew. Chem. Int. Ed. Engl.* 54 (23): 6913–6917.

18 Breit, B. and Seiche, W. (2005). Self-assembly of bidentate ligands for combinatorial homogeneous catalysis based on an A-T base-pair model. *Angew. Chem. Int. Ed. Engl.* 44 (11): 1640–1643.

19 Waloch, C., Wieland, J., Keller, M., and Breit, B. (2007). Self-assembly of bidentate ligands for combinatorial homogeneous catalysis: methanol-stable platforms analogous to the adenine–thymine base pair. *Angew. Chem.* 119 (17): 3097–3099.

20 Weis, M., Waloch, C., Seiche, W., and Breit, B. (2006). Self-assembly of bidentate ligands for combinatorial homogeneous catalysis: asymmetric rhodium-catalyzed hydrogenation. *J. Am. Chem. Soc.* 128 (13): 4188–4189.

21 Wieland, J. and Breit, B. (2010). A combinatorial approach to the identification of self-assembled ligands for rhodium-catalysed asymmetric hydrogenation. *Nat. Chem.* 2 (10): 832–837.

22 Tang, W. and Zhang, X. (2003). New chiral phosphorus ligands for enantioselective hydrogenation. *Chem. Rev.* 103 (8): 3029–3070.

23 Berthod, M., Mignani, G., Woodward, G., and Lemaire, M. (2005). Modified BINAP: the how and the why. *Chem. Rev.* 105 (5): 1801–1836.

24 Miyashita, A., Yasuda, A., Takaya, H. et al. (1980). Synthesis of 2,2′-bis (diphenylphosphino)-1,1′-binaphthyl (BINAP), an atropisomeric chiral bis(triaryl)phosphine, and its use in the rhodium(I)-catalyzed asymmetric hydrogenation of .alpha.-(acylamino)acrylic acids. *J. Am. Chem. Soc.* 102 (27): 7932–7934.

25 Miyashita, A., Takaya, H., Souchi, T., and Noyori, R. (1984). 2, 2'-bis (diphenylphosphino)-1, 1'-binaphthyl(binap). *Tetrahedron* 40 (8): 1245–1253.

26 Wenz, K.M., Leonhardt-Lutterbeck, G., and Breit, B. (2018). Inducing axial chirality in a supramolecular catalyst. *Angew. Chem. Int. Ed. Engl.* 57 (18): 5100–5104.

27 Blum, J., Huminer, H., and Alper, H. (1992). Alkyne hydration promoted by RhCl3 and quaternary ammonium salts. *J. Mol. Catal.* 75 (2): 153–160.

28 Casado, R., Contel, M., Laguna, M. et al. (2003). Organometallic gold(III) compounds as catalysts for the addition of water and methanol to terminal alkynes. *J. Am. Chem. Soc.* 125 (39): 11925–11935.

29 Mizushima, E., Sato, K., Hayashi, T., and Tanaka, M. (2002). Highly efficient AuI-catalyzed hydration of Alkynes. *Angew. Chem. Int. Ed.* 41 (23): 4563–4565.

30 Hartman, J.W., Hiscox, W.C., and Jennings, P.W. (1993). Catalytic hydration of alkynes with platinum(II) complexes. *J. Org. Chem.* 58 (26): 7613–7614.

31 Fukuda, Y. and Utimoto, K. (1991). Effective transformation of unactivated alkynes into ketones or acetals with a gold(III) catalyst. *J. Org. Chem.* 56 (11): 3729–3731.

32 Alvarez, P., Bassetti, M., Gimeno, J., and Mancini, G. (2001). Hydration of terminal alkynes to aldehydes in aqueous micellar solutions by ruthenium(II) catalysis; first anti-Markovnikov addition of water to propargylic alcohols. *Tetrahedron Lett.* 42 (48): 8467–8470.

33 Grotjahn, D.B., Incarvito, C.D., and Rheingold, A.L. (2001). Combined effects of metal and ligand capable of accepting a proton or hydrogen bond catalyze anti-Markovnikov hydration of terminal alkynes. *Angew. Chem. Int. Ed.* 40 (20): 3884–3887.

34 Grotjahn, D.B. and Lev, D.A. (2004). A general bifunctional catalyst for the anti-Markovnikov hydration of terminal alkynes to aldehydes gives enzyme-like rate and selectivity enhancements. *J. Am. Chem. Soc.* 126 (39): 12232–12233.

35 Suzuki, T., Tokunaga, M., and Wakatsuki, Y. (2001). Ruthenium complex-catalyzed anti-Markovnikov hydration of terminal alkynes. *Org. Lett.* 3 (5): 735–737.

36 Tokunaga, M., Suzuki, T., Koga, N. et al. (2001). Ruthenium-catalyzed hydration of 1-alkynes to give aldehydes: insight into anti-Markovnikov regiochemistry. *J. Am. Chem. Soc.* 123 (48): 11917–11924.

37 Tokunaga, M. and Wakatsuki, Y. (1998). The first anti-Markovnikov hydration of terminal alkynes: formation of aldehydes catalyzed by a ruthenium(II)/phosphane mixture. *Angew. Chem. Int. Ed.* 37 (20): 2867–2869.

38 Chevallier, F. and Breit, B. (2006). Self-assembled bidentate ligands for Ru-catalyzed anti-Markovnikov hydration of terminal alkynes. *Angew. Chem. Int. Ed. Engl.* 45 (10): 1599–1602.

39 Green, M.M. and Wittcoff, H.A. (2006). *Organic Chemistry Principles and Industrial Practice*, 1e. Weinheim: Wiley-VCH.

40 Ahmed, T.J., Knapp, S.M.M., and Tyler, D.R. (2011). Frontiers in catalytic nitrile hydration: Nitrile and cyanohydrin hydration catalyzed by homogeneous organometallic complexes. *Coord. Chem. Rev.* 255 (7-8): 949–974.

41 Kukushkin, V.Y. and Pombeiro, A.J.L. (2002). Additions to metal-activated organonitriles. *Chem. Rev.* 102 (5): 1771–1802.

42 Trost, B.M. (2002). On inventing reactions for atom economy. *Acc. Chem. Res.* 35 (9): 695–705.

43 Šmejkal, T. and Breit, B. (2007). Self-assembled bidentate ligands for ruthenium-catalyzed hydration of nitriles. *Organometallics* 26 (9): 2461–2464.

44 Usui, I., Schmidt, S., Keller, M., and Breit, B. (2008). Allylation of N-heterocycles with allylic alcohols employing self-assembling palladium phosphane catalysts. *Org. Lett.* 10 (6): 1207–1210.

45 Trost, B.M. and Crawley, M.L. (2003). Asymmetric transition-metal-catalyzed allylic alkylations: applications in total synthesis. *Chem. Rev.* 103 (8): 2921–2944.

46 Fleming, F.F. (1999). Nitrile-containing natural products. *Nat. Prod. Rep.* 16 (5): 597–606.

47 Larock, R.C. (1999). *Comprehensive Organic Transformations: A Guide to Functional Group Preparations*, 2e. New York, NY: Wiley-VCH.

48 Torborg, C. and Beller, M. (2009). Recent applications of palladium-catalyzed coupling reactions in the pharmaceutical, agrochemical, and fine chemical industries. *Adv. Syn. Catal.* 351 (18): 3027–3043.

49 Zhang, H., Su, X., and Dong, K. (2020). Recent progress in transition-metal-catalyzed hydrocyanation of nonpolar alkenes and alkynes. *Org. Biomol. Chem.* 18 (3): 391–399.

50 Goertz, W., Kamer, P.C.J., van Leeuwen, P.W.N.M., and Vogt, D. (1997). Application of chelating diphosphine ligands in the nickel-catalysed hydrocyanation of alk-l-enes and ω-unsaturated fatty acid esters. *Chem. Commun.* (16): 1521–1522.

51 Freixa, Z. and van Leeuwen, P.W.N.M. (2003). Bite angle effects in diphosphine metal catalysts: steric or electronic? *Dalton Trans.* (10): 1890–1901.

52 Goertz, W., Keim, W., Vogt, D. et al. (1998). Electronic effects in the nickel-catalysed hydrocyanation of styrene applying chelating phosphorus ligands with large bite angles. *J. Chem. Soc., Dalton Trans.* (18): 2981–2988.

53 Kranenburg, M., Kamer, P.C.J., van Leeuwen, P.W.N.M. et al. (1995). Effect of the bite angle of diphosphine ligands on activity and selectivity in the nickel-catalysed hydrocyanation of styrene. *J. Chem. Soc., Chem. Commun.* (21): 2177.

54 de Greef, M. and Breit, B. (2009). Self-assembled bidentate ligands for the nickel-catalyzed hydrocyanation of alkenes. *Angew. Chem. Int. Ed. Engl.* 48 (3): 551–554.